

PHOTOMETRIC EVOLUTION OF ELLIPTICAL GALAXIES

JUNG, HEE AND LEE, SEE-WOO

Department of Astronomy, Seoul National University

(Received Oct. 4, 1994; Accepted Oct. 18, 1994)

ABSTRACT

We have examined the photometric evolution of elliptical galaxies, using stellar evolutionary models covering the wide ranges of metallicity and mass, and the different IMFs (simple IMF & time-dependent bimodal IMF). The model with a time-dependent bimodal IMF can reproduce the observed integrated magnitudes and colors at all wavelengths.

The computed model shows that the star formation in elliptical galaxies is still going on, although the number of newly born stars is very small. The chemical evolutionary effect is clearly seen in the C-M diagram of computed elliptical galaxies.

Key Words : elliptical galaxies, photometric properties, photometric evolution

I. INTRODUCTION

Galaxies show diverse integrated photometric properties (integrated magnitudes and colors) which are related to different star formation history and different stellar population as well as metallicity. To explain these observed photometric properties, the evolutionary population synthesis method has been used since the pioneer work of Tinsley(1972).

Most of the previous population synthesis models for elliptical galaxies are constructed on the assumption that all the stars evolve along the evolutionary tracks with the solar abundance ($Z=0.02$) (Tinsley 1968,1972,1978; Searle *et al.* 1973; Tinsley & Gunn 1976; Huchra 1977; Bruzual 1983; Charot & Bruzual 1991; Bruzual & Charot 1993). And even the model constructor who consider the metallicity effect due to chemical evolution (Arimoto & Yoshii 1986, 1987), used inconsistent evolutionary tracks without considering the evolution after the giant phase.

So we have constructed a photometric evolutionary model of elliptical galaxies taking into account the time variation of metallicity during chemical evolution. And stellar evolutionary models which cover the wide ranges of metallicity and mass and include the post red giant branch phase are used. Moreover, two different forms of IMF (simple IMF & time-dependent bimodal IMF) are applied. From the constructed photometric evolution model for elliptical galaxies, we examined in detail the star formation history and the properties of constituent stellar population and metallicities.

In §2, the method of model construction for chemical evolution and adopted evolutionary models are described. The results for different two forms of IMF are described in section §3. The conclusion and discussion are presented in the last section.

II. MODEL CONSTRUCTION

(a) Basic Equations for Chemical Evolution

We assume that a galaxy is a closed system, and the gas is quickly mixed after being ejected from dying stars. Then, the basic equations for chemical evolution are given by

$$\frac{d\rho_s(t)}{dt} = \psi(t) - E_g(t), \quad (1)$$

$$\frac{d\rho_g(t)}{dt} = -\psi(t) + E_g(t), \quad (2)$$

$$\frac{dZ(t)}{dt} = (E_Z - ZE_g) / \rho_g, \quad (3)$$

where ρ_s , ρ_g , Z are stellar density, gas density, and metal abundance in gas, respectively. $\psi(t)$ is star formation rate(SFR), $E_g(t)$ and $E_z(t)$ are respectively, ejected gas and ejected metal abundance from dying stars. The latter are given by

$$E_g(t) = \int_{m_l}^{m_u} (m - \omega_m) \phi(m, t - \tau_m) \psi(t - \tau_m) dm, \quad (4)$$

$$E_z(t) = \int_{m_l}^{m_u} (m - \omega_m - \delta m_z) \phi(m, t - \tau_m) \psi(t - \tau_m) Z(t - \tau_m) dm \\ + \int_{m_l}^{m_u} \delta m_z \phi(m, t - \tau_m) \psi(t - \tau_m) dm \quad (5)$$

where m_l is the mass of a star whose lifetime(τ_m) is equal to t , and m_u and m_l are, respectively, the upper and lower mass limits, and ω_m is the mass of remnant of stars with mass m . ϕ is the IMF, and δm_z is the amount of newly synthesized metals in stars with mass m . The data for ω_m and δm_z are taken from Renzini & Voli(1981) and Tosi & Diaz(1985).

We adopt a SFR proportional to a power of gas density as suggested by Schmidt(1963),

$$\psi(t) = \mu \rho_g^n. \quad (6)$$

Two forms of IMF are considered. One is a simple IMF of Salpeter (1955), and the other is a time-dependent bimodal IMF of Lee & Chun (1986). Each form of two IMFs are as follows;

$$\phi(m) = \phi_o m^{-x}, \quad (7)$$

$$\xi(\log m, t) = \xi_o(t) [\omega_1 \xi_1(\log m, t) + \omega_2 \xi_2(\log m, t)], \\ \xi_i(\log m) = \exp[-B_i(\log m - C_i)^2] \\ + \left(\frac{m}{H_i}\right)^{\gamma_i} \exp[-E_i\left(\frac{m}{H_i}\right)^{\beta_i} A(t)], \quad (8)$$

$$A(t) = \frac{1}{1 - (1/D) \exp[-(t - t_o)^2/\delta^2]},$$

where normalization constants ϕ_o and $\xi_o(t)$ are defined by the following normalization conditions ;

$$\int_{m_l}^{m_u} m \phi(m) dm = 1, \quad \int_{m_l}^{m_u} m \xi(\log m, t) dm = 1, \quad (9)$$

where the lower and upper mass limits are taken as $m_l(= 0.1m_\odot)$ and $m_u(= 150m_\odot)$. The constants in eq.(7) and (8) will be determined by observational constraints.

(b) Data Sets of Stars

i) Evolutionary Models

We have compiled evolutionary tracks for $Z = 0.001, 0.004, 0.008, 0.02,$ and 0.04 in the mass range of $0.04 \sim 120 m_\odot$ as seen in Table 1. The high mass stars ($\geq 7M_\odot$) are evolved up to the C-burning stage, and stars of $0.8 \sim 5 M_\odot$ are evolved up to the asymptotic giant branch stage. Particularly, for the stars of $0.8 \sim 1.7 M_\odot$, the Dorman's model(1992) is applied after the He-flash. The low mass stars ($\leq 0.8M_\odot$) are at the H-burning stage.

Table 1. Sources of Evolutionary Models.

Mass range	Stellar evolutionary tracks	Reference
$7 \sim 120 m_{\odot}$	ZAMS \rightarrow C-burning	Schaller <i>et al.</i> (1992) $Z = 0.001, 0.02$
$2 \sim 5 m_{\odot}$	ZAMS \rightarrow AGB	Charbonnel <i>et al.</i> (1992) $Z = 0.004$
$0.8 \sim 1.7 m_{\odot}$	ZAMS \rightarrow He flash	Schaerer <i>et al.</i> (1992) $Z = 0.008, 0.04$
$0.8 \sim 1.7 m_{\odot}$	ZAHB \rightarrow AGB	Dorman(1992)
$0.04 \sim 0.8 m_{\odot}$	ZAMS \rightarrow H-burning	Sweigart & Gross(1978), Mengel <i>et al.</i> (1979), VandenBerg <i>et al.</i> (1985)

Table 2. Stellar Atmospheric Models.

Photometric properties	Reference
(B-C), (B-V), (U-B)	Buser & Kurucz (1978) VandenBerg & Bell (1978) ($\log T_e < 3.75$, LC V) Bell & Gustafsson (1978) ($\log T_e < 3.75$, LC I, III)
(V-R), (V-J), (V-K)	Johnson (1966)

ii) Photometric Calibrations

To compute the colors of synthetic stellar population, the photometric calibrations of effective temperature and luminosity are needed. These parameters are transformed to absolute visual magnitude and various colors by using the atmosphere models in Table 2.

For given SFR and IMF, the number of stars born with mass m_j at time t_i is given by

$$N_j(t_i, m_j) = M_G \int_{t_{i-}}^{t_{i+}} \int_{m_{j-}}^{m_{j+}} \psi(t) \phi(m) dm dt, \quad (10)$$

where $M_G (= 5 \times 10^{12} m_{\odot})$ is the total mass of galaxy. Here we assume that the stars in the mass interval of $m_{j-} (= \sqrt{m_{j-1} m_j}) \sim m_{j+} (= \sqrt{m_j m_{j+1}})$ and in the time interval of $t_{i-} (= \sqrt{t_{i-1} t_i}) \sim t_{i+} (= \sqrt{t_i t_{i+1}})$ correspond to the stars with mass m_j born at time t_i . These stars evolve along the relevant evolutionary tracks of metallicity $Z(t_i)$, contributing to the integrated light and colors of the galaxy at a certain galactic age. Hence the integrated luminosity and colors of a galaxy at galactic age t_G can be deduced by summing up the contribution of light and colors by all stars which were born before t_G .

III. RESULTS

The main computations for photometric evolution of elliptical galaxies have been done for each of simple IMF and time-dependent bimodal IMF.

1. Simple IMF

To examine the metallicity effect, we have computed the two cases with a simple IMF ; One is the constant metallicity ($Z = Z_{\odot}$) and the other is for a variable metallicity with time.

Figure 1 shows the computed colors at 15Gyr by changing the value of IMF index x . For the constant Z model, all colors become redder monotonically as x increases. But for the varying Z model, the results are more complicated as compared with the constant Z model. For $x < 2$ ($x > 2$), the stellar metallicity has a value above (below) Z_{\odot} , so the varying Z model shows bluer (redder) color than the constant Z model for $x < 2$ ($x > 2$). It is noted that the varying Z model with a simple IMF can not reproduce the observed value at all colors for any value of IMF index x .

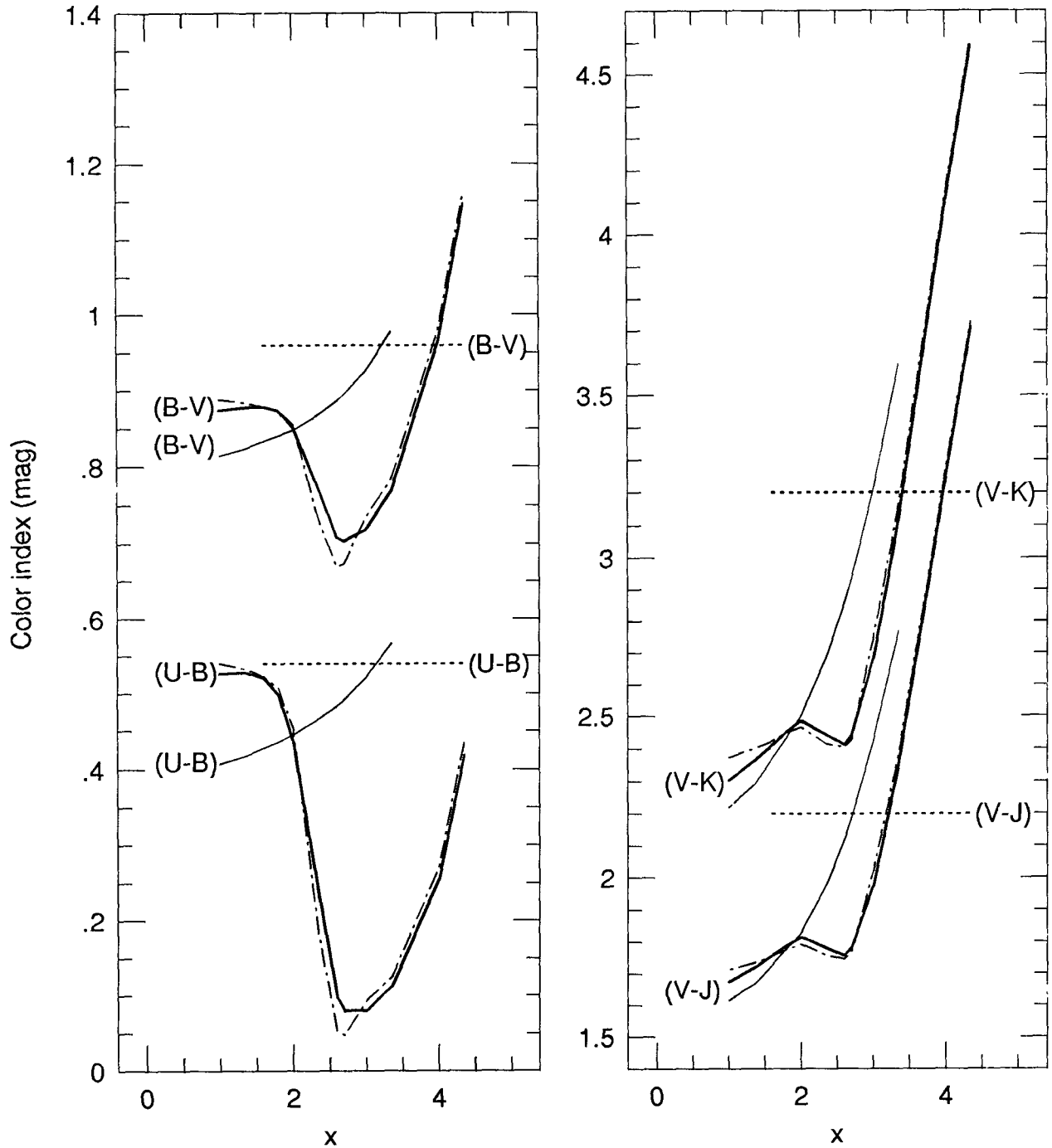


Fig. 1. Computed colors at galactic age 15Gyr with changing simple IMF index x . Thin solid lines represent the constant $Z(= Z_{\odot})$ model, dot-dashed lines and thick solid lines denote the varying Z model, with the SFR index μ is 1 and 10, respectively ($n=1$). Dotted lines are the observed value of Sandage(1973).

(b) Time - Dependent Bimodal IMF

We can find two models with a time-dependent bimodal IMF, which reproduce the observed colors at all wavelengths at galactic age 15Gyr, taking $\mu = 10$ and $n = 1$ in eq.(6) for SFR. More detailed results for these two models are as follows.

i) Form of IMFs

Two bimodal IMFs (A and B models) are shown in Figure 2. Their main characteristics are the increase of the number of low mass stars with time. The IMF of model B is set to have a larger number of low mass stars at the early evolutionary stage than in the case of model A.

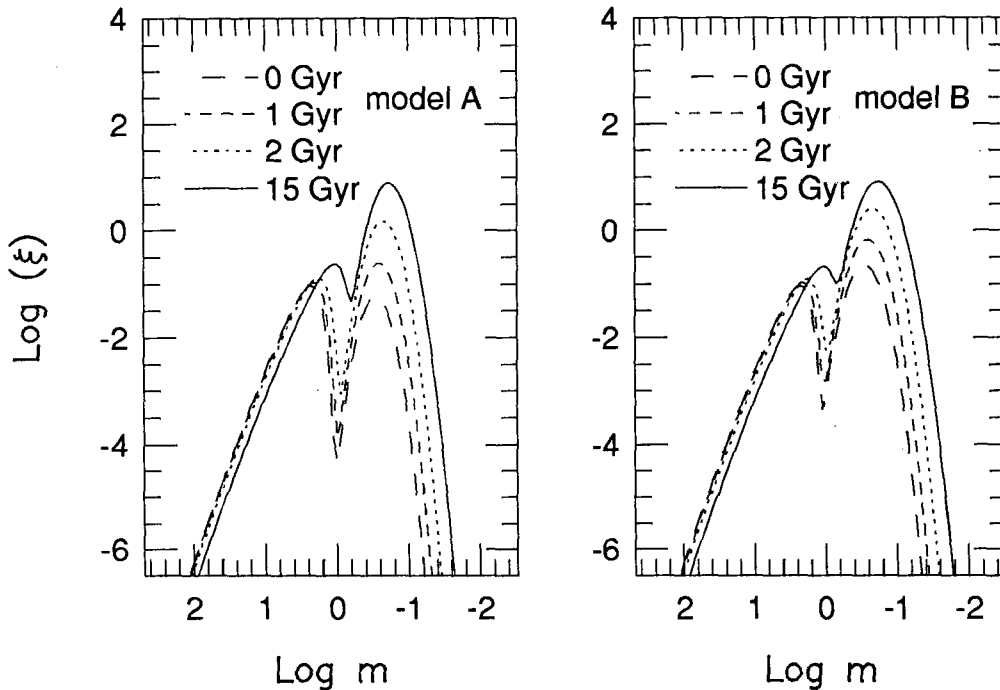


Fig. 2. The temporal variation of adopted time-dependent bimodal IMF.

ii) Results for Chemical Evolution

The temporal variations of some physical parameters are shown in Figure 3, where dotted and solid lines denote models A and B, respectively. The two models show nearly similar tendency with time. The most of stars are born within 2Gyr and the metallicity increases abruptly up to $[\text{Fe}/\text{H}] \sim 0.6$ during the very early phase (1Gyr) of the evolution. Since the model B have a larger number of low mass stars at the early phase (Figure 2), the amounts of the ejected gas (E_g) and metals (E_Z) from dying stars, and the metallicity in the model B are smaller than in the case of the model A, leading to the smaller gas density and lower SFR.

iii) Temporal Variation of Integrated Magnitude and Colors

Figure 4 shows the temporal variation of integrated magnitude and colors of a synthetic elliptical galaxy. At the galactic age $t_G (=15\text{Gyr})$, they show a good agreement with the observed values of M_V and all colors which are denoted by the limited bars in Figure 4. Absolute magnitude reaches the maximum brightness abruptly within the galactic time 0.2Gyr by the rapid star formation, and then become fainter slowly. The integrated colors become bluest abruptly within 0.1Gyr and then redder rapidly until $t \approx 1\text{Gyr}$ and after that the colors become redder slowly with time. The temporal variations of integrated magnitude and colors in the C-M diagram are shown in Figure 5, where filled circles at the rightside are observed values of elliptical galaxies (Persson et al. 1979). The temporal

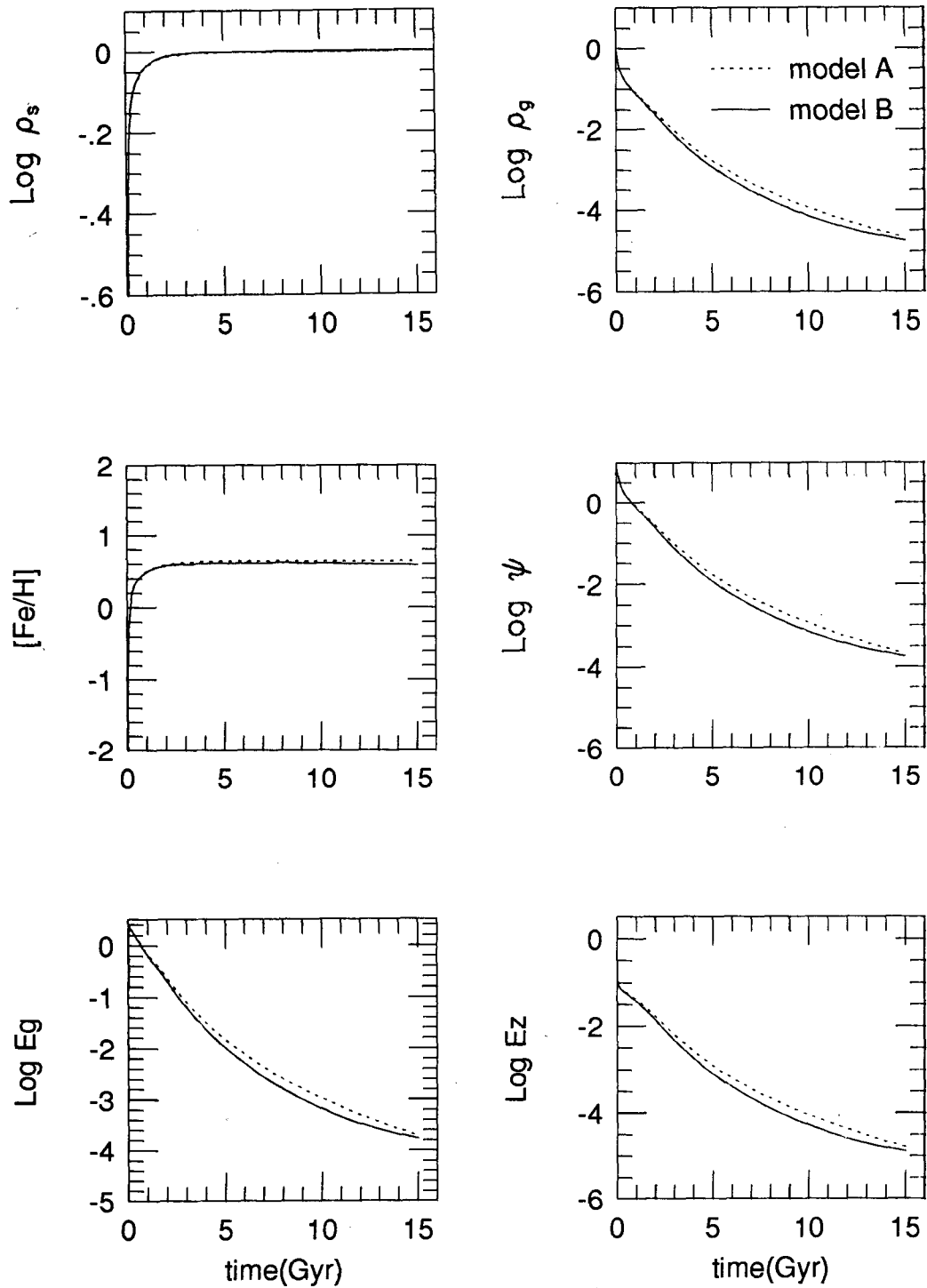


Fig. 3. The temporal variation of physical parameters. Dotted lines and solid lines correspond to model A and B, respectively.

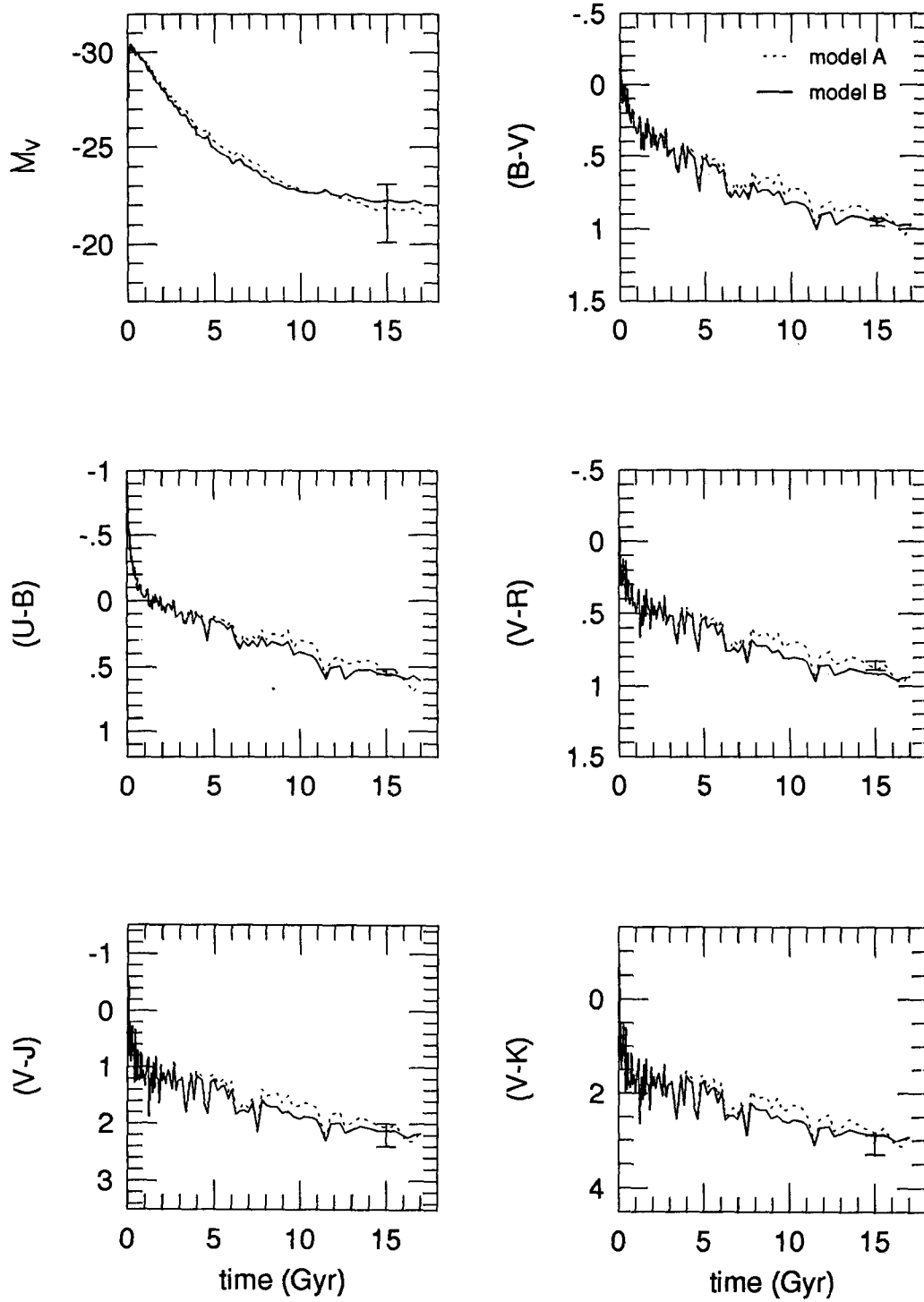


Fig. 4. Evolution of photometric properties (absolute magnitudes and colors).

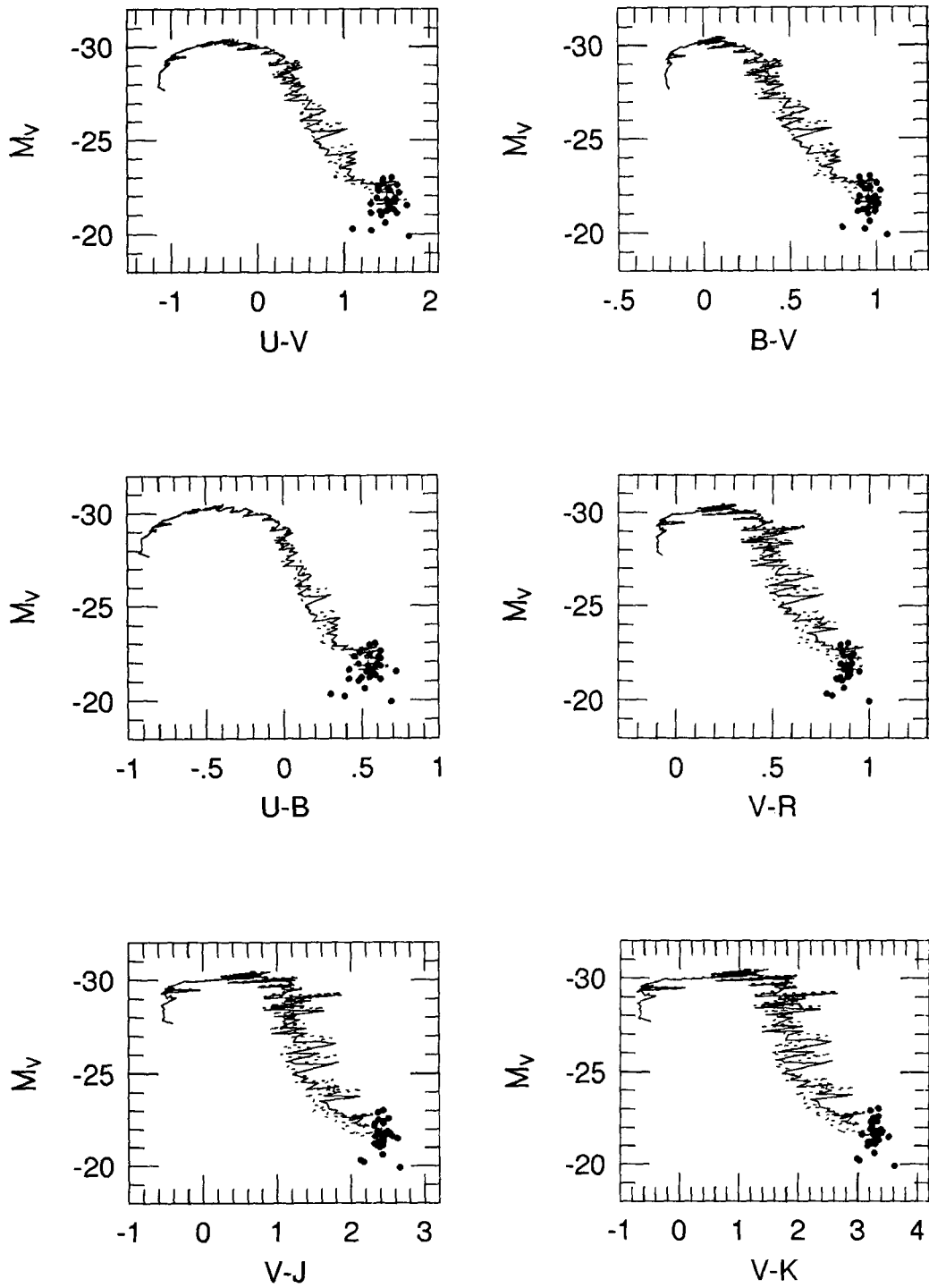


Fig. 5. Evolution of photometric properties in C-M diagram (from the left top to the right bottom of each Figure). Filled circles are observed values of elliptical galaxies (Persson et al. 1979).

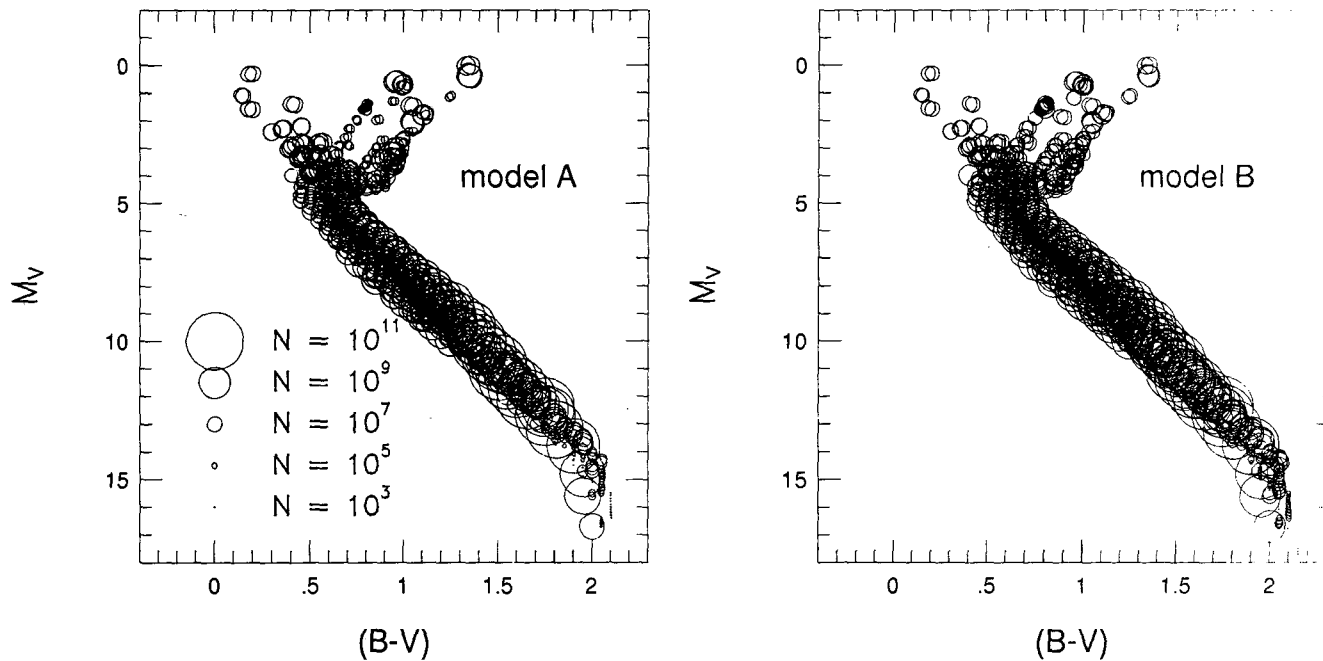


Fig. 6. C-M diagram of all stars at galactic age 15Gyr.

variations of some characteristics of synthetic galaxy such as the number of all stars, total luminosity, total mass of stars, M_V and colors are shown in Table 3.

iv) Color - Magnitude Diagram

The C-M diagram of all stars in the synthetic elliptical galaxies at the galactic age of 15Gyr are shown in Figure 6 for the models A and B. The size of circles is proportional to the logarithmic value of the number of stars. The stars with the bluest colors ($0.1 \leq (B-V) \leq 0.3$) in Figure 6 are the main sequence stars whose mass is in the range of $1.7 \sim 2.5m_{\odot}$ and age is about 0.5 Gyr. The existence of these stars implies that the star formation is still going on in the elliptical galaxies. But as shown in Table 4 the number of these newly born stars and their total luminosity are very small as compared with the total values of the whole galaxy.

The elliptical galaxies have been thought as quiescent galaxies whose star formation had ceased long time ago. But dwarf ellipticals in the local group are known to have undergone recent star formation (Freedman 1991). The connection between dwarf ellipticals and normal ellipticals including giant ellipticals is not yet known well. And there is no direct evidence that the star formation is occurring in normal ellipticals as in the local group dwarf ellipticals. But a number of ellipticals are now known to have detectable amounts of interstellar medium (see reviews by Schweizer 1987, Jura 1988). The existence of sources for star formation -interstellar medium- suggests a possibility of star forming in ellipticals as long as no strong depleting mechanism such as a galactic wind is operating in the ellipticals.

The most of stars in the synthetic ellipticals in Figure 6 are at the MS stage which has a magnitude width of $\Delta M_V \simeq 2$ mag. and a color width of $\Delta(B-V) \simeq 0.4$ at $(B-V) \simeq 1$. The significant width of the MS is mainly due to the chemical evolutionary effect. That is, the brighter and redder MS stars have higher metal abundance and younger age than the fainter and bluer MS stars.

v) Color Distribution of Stars

Figure 7 shows the number fraction(a) and the luminosity fraction(b) of dwarfs and giants against (B-V) color.

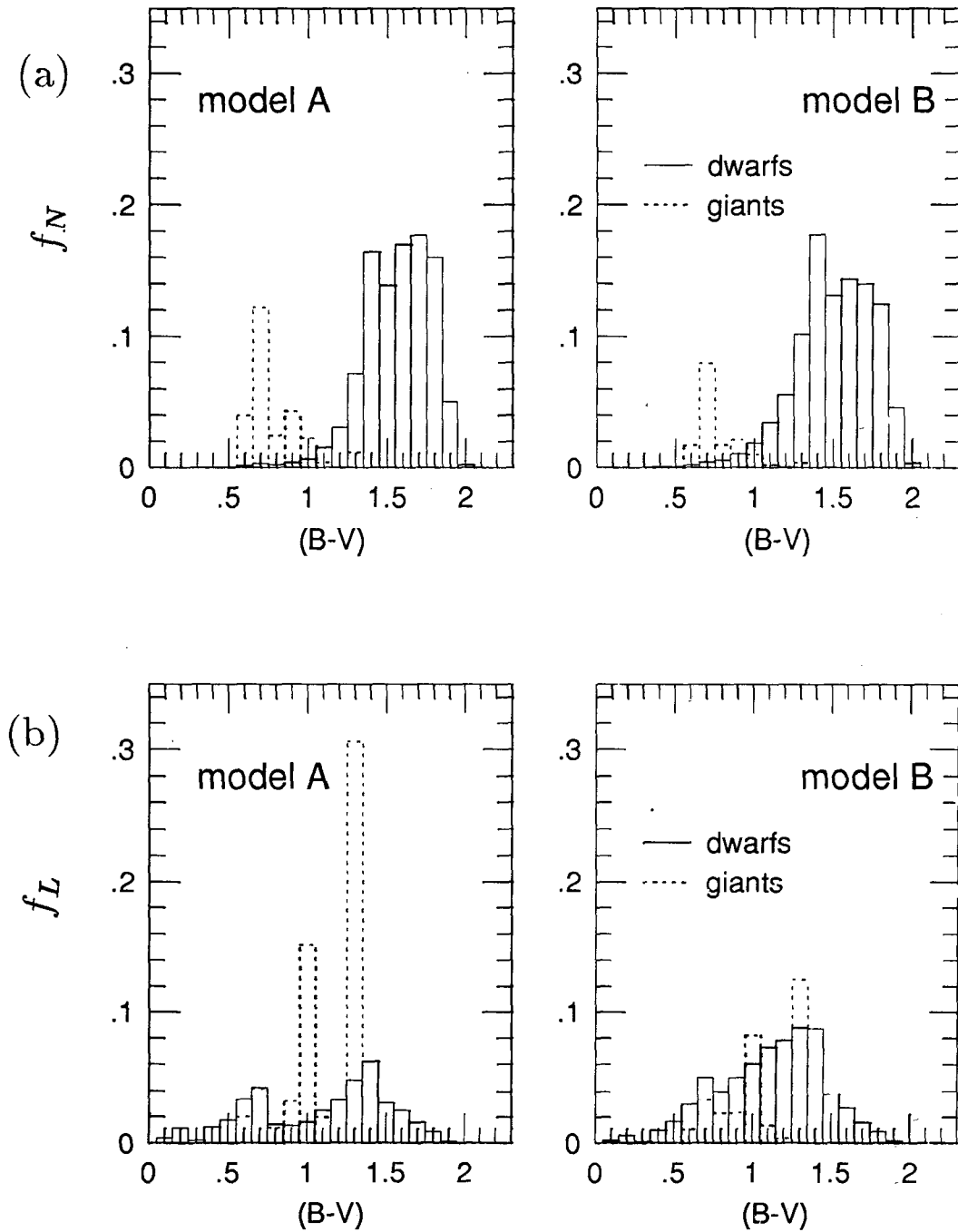


Fig. 7. The number fraction(a) and the luminosity fraction(b) of dwarfs and giants against (B-V). For visualizing, the number fraction of giants is multiplied by 100.

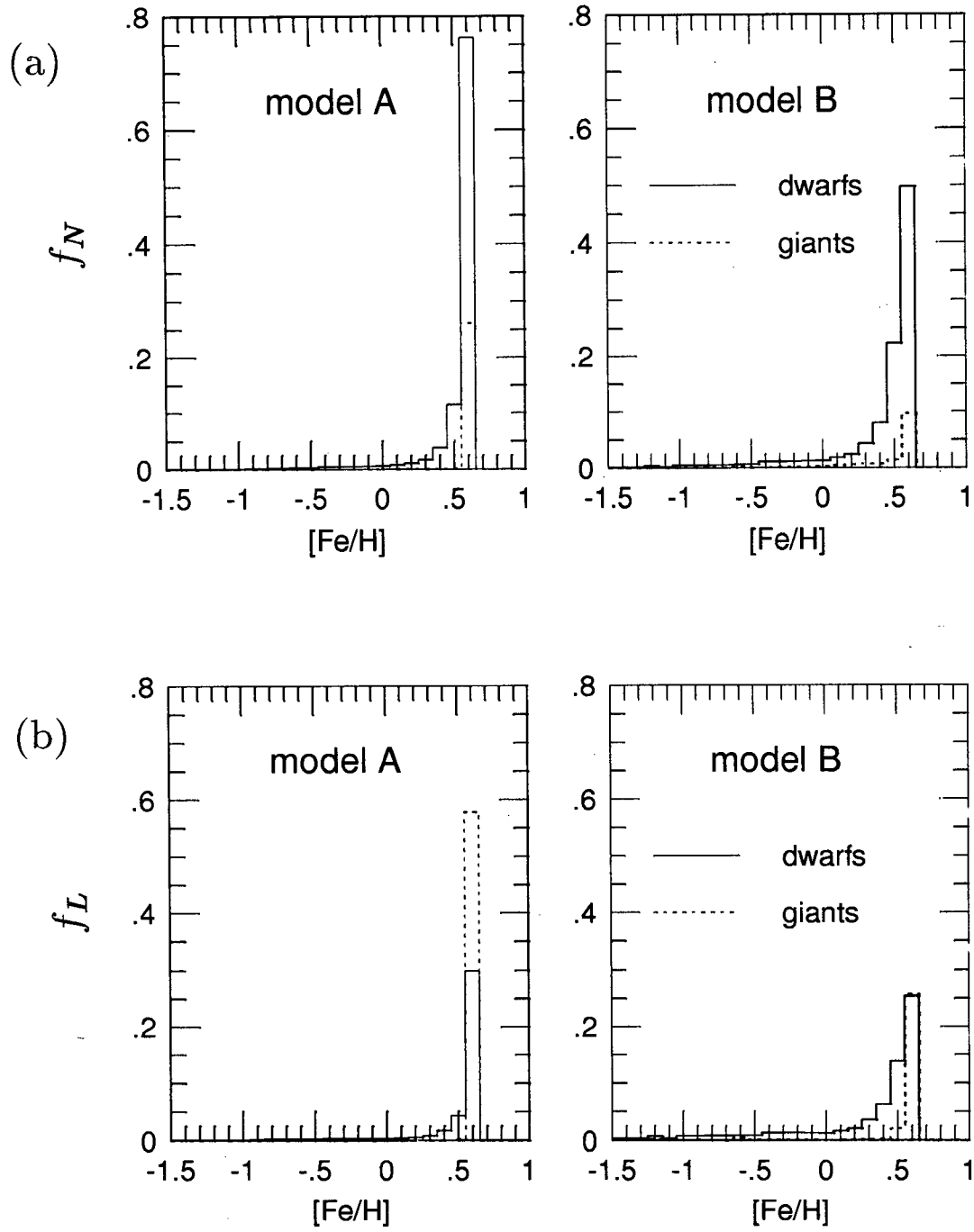


Fig. 8. Distribution of the number and integrated light of dwarfs and giants against $[Fe/H]$. For visualizing, the number fraction of giants is multiplied by 100.

Table 3. Temporal Variation of Some Characteristics of Synthetic Galaxy.

Parameters	Model	0.1 Gyr	1 Gyr	6 Gyr	15 Gyr
Number of all stars	A	6.94×10^{11}	1.24×10^{12}	1.51×10^{12}	1.55×10^{12}
	B	6.81×10^{11}	1.77×10^{12}	2.76×10^{12}	4.28×10^{11}
Total luminosity	A	$3.51 \times 10^{14} L_{\odot}$	$7.20 \times 10^{13} L_{\odot}$	$6.13 \times 10^{11} L_{\odot}$	$7.91 \times 10^{10} L_{\odot}$
	B	3.44×10^{14}	6.75×10^{13}	4.63×10^{11}	1.10×10^{11}
Total mass of stars	A	$2.34 \times 10^{12} M_{\odot}$	$2.36 \times 10^{12} M_{\odot}$	$5.02 \times 10^{11} M_{\odot}$	$4.28 \times 10^{11} M_{\odot}$
	B	2.30×10^{12}	2.44×10^{12}	8.94×10^{11}	8.45×10^{11}
Mv	A	-30.203	-29.488	-24.537	-21.923
	B	-30.180	-29.424	-24.181	-22.274
(B-V)	A	0.018	0.332	0.543	0.944
	B	0.019	0.339	0.594	0.954
(U-B)	A	-0.540	-0.031	0.151	0.571
	B	-0.540	-0.025	0.186	0.569

Table 4. Number & Luminosity Fractions of Stars which were born during the given Galactic Time.

Galactic time	Model A		Model B	
	f_n^1	f_L^2	f_n^1	f_L^2
14.5 ~ 15 Gyr	0.07 %	2.00 %	0.03 %	1.02 %
14 ~ 15	0.14	2.89	0.07	1.49
10 ~ 15	1.25	14.60	0.55	6.40

¹number fraction²luminosity fraction

Table 5. Contribution of Dwarfs and Giants in Number and Luminosity

Model	n_d^1	n_g^2	L_d^3	L_g^4
A	99.73 %	0.27 %	41.57 %	58.43 %
B	99.85	0.15	68.37	31.63

¹number fraction of dwarfs²number fraction of giants³luminosity fraction of dwarfs⁴luminosity fraction of giants

Even though the number fraction of giants is very small as compared with dwarfs, their luminosity fraction is significant. Hence the giants in the model A contribute about 60% of the total luminosity as seen in Table 5. But in the model B, the giants contribute only one third of the total luminosity. The less contribution of giants as compared with dwarfs is due to the formation of more low mass stars at the early stage of the evolution in the model B.

vi) Metallicity Distribution of Stars

The distribution of the number and integrated light of dwarfs and giants are shown against [Fe/H] in Figure 8. The most of stars have [Fe/H] ≈ 0.6 which is equivalent to the age of 14Gyr, and hence the most of total luminosity is contributed by these stars as seen in Figure 8. The number fraction of stars with [Fe/H] < -2 and [Fe/H] < 0 in the model A(B) are 0.25% (0.61%) and 4.21% (10.02%), respectively. The stars with low metal abundance ([Fe/H] < 0) are all at the MS stage and their mass is less than $1m_{\odot}$. Accordingly their contribution to the total luminosity is only 3.95% (17.64%) in the model A(B).

IV. CONCLUSION AND DISCUSSION

We have calculated the photometric evolution of elliptical galaxies, taking into account the temporal variation of metallicity during the chemical evolution and the different IMFs (simple IMF & time-dependent bimodal IMF).

In the model with a simple IMF, colors do not become redder monotonically as the value of IMF index x increases. By the model with a simple IMF, the observed photometric properties of elliptical galaxies can not be reproduced. However, the models with a time-dependent bimodal IMF can reproduce well the observed colors at the galactic age of 15Gyr, showing the following properties of elliptical galaxies ; (i) The most of stars are born within 2Gyr and the metallicity increases abruptly up to $[Fe/H] \sim 0.6$ during the very early phase (1Gyr) of the evolution. (ii) The integrated color of synthetic galaxy become bluest at 0.1Gyr and then redder with time. The integrated magnitude become brighter at ~ 0.2 Gyr and then fainter with time. The maximum brightness ($M_V \simeq -30$) is about 2500 times of the present value. It is noted that some quasars have bluest colors and brightest luminosity like as the early phase of these synthetic galaxies (see data in Véron-Cety & Véron 1993). (iii) The star formation is still going on, although the number of stars which are born during the period of 1Gyr from the present time, is very small (~ 0.1 % of the total number of stars). Their result is very positive for the recent observations for star formation (Freedman 1991) and interstellar medium (Schweizer 1987, Jura 1988). (iv) The significant effect of metallicity spread is shown in the considerable width of the main sequence on the C-M diagram. (v) The contribution of giants to the total luminosity is about 32 ~ 58 % and the average metallicity is about $2.8 \sim 3.9 Z_{\odot}$ which correspond to the observed range in giant elliptical galaxies (Faber 1972, Pagel & Edmunds 1981, O'Connell 1986). For elliptical galaxies, no detailed information except for the integrated colors and magnitude has not been known, and consequently the contribution of giants to the total luminosity can not be correctly estimated in the present study.

REFERENCES

- Arimoto, N., & Yoshii, Y. 1986, *A&A*, 164, 260
 Arimoto, N., & Yoshii, Y. 1987, *A&A*, 173, 23
 Bell, R. A., & Gustafson, B. 1978, *A&AS*, 34, 229
 Bruzual, A. 1983, *ApJ*, 273, 105
 Bruzual, A., & Charot, S. 1993, *ApJ*, 405, 538
 Buser, R., & Kurucz, R. L. 1978, *A&A*, 70, 555
 Charbonnel, C., Meynet, G., Maeder, A., Schaller, G., & Schaerer, D. 1993, *A&AS*, 101, 415
 Charot, S., & Bruzual, A. 1991, *ApJ*, 367, 126
 Dorman, B. 1992, *ApJS*, 81, 221
 Faber, S. M. 1972, *A&A*, 20, 361
 Freedman, W. L. 1991, in *IAU Symp. 149, The Stellar Populations of Galaxies*, ed. B. Barbuy & A. Renzini (Dordrecht: Kluwer), 169
 Huchra, J. P. 1977, *ApJ*, 217, 928
 Johnson, H. L. 1966, *ARA&A*, 4, 193
 Jura, M. 1988, in *Multiwavelength Astrophysics*, 267
 Lee, S.-W., & Chun, M.-Y. 1986, *JKAS*, 19, 51
 Mengel, J. G., Swigart, A. V., Demarque, P., & Gross, P. G. 1979, *ApJS*, 40, 733
 O'Connell, R. W. 1986, in *stellar Populations*, ed. C. Norman, A. Renzini, & M. Tosi (Cambridge : Cambridge Univ. Press), 167
 Pagel, B. E. J., & Edmunds, M. G. 1981, *ARAA*, 19,77
 Persson, S. E., Frogel, J. A., & Aaronson, M. 1979, *ApJS*, 39, 61
 Renzini, A., & Voli, M. 1981, *A&A*, 94, 175
 Salpeter, E. E. 1955, *ApJ*, 121, 161
 Sandage, A. 1973, *ApJ*, 121, 161
 Schaerer, D., Meynet, G., Maeder, A., & Schaller, G. 1993a, *A&AS*, 98, 523

- Schaerer, D., Charbonnel, C., Meynet, G., Maeder, A., Schaller, G., 1993b, A&AS, 102, 339
Schaller, G., Schaerer, D., Meynet, G., Maeder, G., & Maeder, A. 1992, A&AS, 96, 269
- Schmidt, M. 1963, ApJ, 137, 758
- Schweizer, F. 1987, in IAU Symp. 127, Structure and Dynamics of Elliptical Galaxies, ed. de Zeeuv, 109
- Searle, L., Sargent, W. L., & Bagnuolo, W. G. 1973, ApJ, 179, 427
- Sweigart, A. V., & Gross, P. G. 1978, ApJS, 36, 405
- Tinsley, B. M. 1968, ApJ, 151, 547
- Tinsley, B. M. 1972, A&A, 20, 383
- Tinsley, B. M. 1978, ApJ, 222, 14
- Tinsley, B. M., & Gunn, J. E. 1976, ApJ, 203, 52
- Tosi, M., & Diaz, A. I. 1985, MNRAS, 217, 571
- VandenBerg, D. A., & Bell, R. A. 1985, ApJS, 58, 561
- Véron-Cety, M. P. & Véron, P. 1993, A Catalogue of Quasars and Active Galaxies, 6th ed., European Southern Observatory, Scientific report No. 13